PROCEEDINGS OF SPIE

SPIEDigitalLibrary.org/conference-proceedings-of-spie

Impact of phase modulation on the performance of photonic delay-based reservoir computing with semiconductor lasers

Ian Bauwens, Krishan Harkhoe, Peter Bienstman, Guy Verschaffelt, Guy Van der Sande

Ian Bauwens, Krishan Harkhoe, Peter Bienstman, Guy Verschaffelt, Guy Van der Sande, "Impact of phase modulation on the performance of photonic delay-based reservoir computing with semiconductor lasers," Proc. SPIE 12143, Nonlinear Optics and its Applications 2022, 121430L (25 May 2022); doi: 10.1117/12.2626778

SPIE.

Event: SPIE Photonics Europe, 2022, Strasbourg, France

Impact of phase modulation on the performance of photonic delay-based reservoir computing with semiconductor lasers

Ian Bauwens[a], Krishan Harkhoe[a], Peter Bienstman[b], Guy Verschaffelt[a], and Guy Van der Sande[a]

[a]Applied Physics Research Group, Vrije Universiteit Brussel, Pleinlaan 2, 1050 Brussels, Belgium

[b]Photonics Research Group, Department of Information Technology, Ghent University-IMEC, Technologiepark Zwijnaarde 126, 9052 Ghent, Belgium

ABSTRACT

In photonic reservoir computing, semiconductor lasers with delayed feedback have been used to efficiently solve difficult and time-consuming problems. The injection of data in these systems is often performed optically into the reservoir. Based on simulations, we show that the performance depends heavily on the way that information is encoded in this optical injection signal. In the simulations, we compare various input configurations consisting of Mach-Zehnder modulators and phase modulators for injecting the signal. We observe far better performance in our results, see also [Bauwens et al, Opt. Express 30, 13434 (2022)], on a one-step ahead time-series prediction task when modulating the phase of the injected signal rather than only modulating its amplitude.

Keywords: Photonics, delay-based, reservoir computing, phase modulation, semiconductor lasers

1. INTRODUCTION

In our current technological society, we are becoming increasingly able to process and analyze information using machine learning.[1] The concept of reservoir computing (RC) within this machine learning field offers a simple, yet powerful technique to use recurrent networks for computing. RC systems have shown good performance in various benchmark tasks, such as speech recognition,[2–4] non-linear channel equalization[5] or time-series predictions.[6–8] An RC system consists of a large recurrent neural network with fixed interconnections. Its topology can be described in three separate components: an input layer, the reservoir, and an output layer. In the input layer, the data is injected into the system and is sent to the reservoir, which consists of a recurrently connected network of non-linear nodes (i.e. neurons). The processed information is then sent to the output layer, where the output weights are optimized to match the output with a corresponding target output. The optimization of weights, and thus the training phase, occurs only in the output layer, whereas the internal weights of the reservoir itself are not altered. This makes training much more straightforward compared to other artificial neural networks (such as deep artificial networks, that also require training of the network's internal nodes) and simplifies reservoir computing in its implementation. Interesting implementations of RC systems can be found in the emerging field of neuromorphic photonics. The advantages of using photonic systems are abundant, ranging from a low-energy consumption, high-speed performance and the possibility of high inherent parallelism.[9,10]

There already exist several successful implementations of photonic RC systems, e.g. based on a network of passive elements or semiconductor optical amplifiers,[11–14] by using a diffractive optical element coupled to a network of vertical cavity surface emitting lasers[15] or by using excitable photonic systems (also referred to as spiking systems).[16,17] In this paper, we focus on a single mode semiconductor laser with delay-based RC.[5,18–23] The injection of input data into this reservoir can be performed via several methods. The input data can e.g. be injected electronically by direct modulation of the injection current.[24] In this work, however, we will focus on optically injected data, which has the advantage of allowing higher data injection rates.[25] This latter method can be performed by modulating the phase of the injected electric field by using a phase modulator or by modulating the amplitude of the electric field.[19,26–29] Although these various injection schemes will have an effect on the final performance of RC, their influence on RC performance has not yet been studied and compared in detail. In

Further author information: (Send correspondence to Ian Bauwens)
Ian Bauwens: E-mail: ian.bauwens@vub.be

Nonlinear Optics and its Applications 2022, edited by Neil G. R. Broderick, John M. Dudley, Anna C. Peacock, Proc. of SPIE Vol. 12143, 121430L · © 2022 SPIE
0277-786X · doi: 10.1117/12.2626778

this work, we numerically investigate the effect of the optical data injection configurations on the performance of delay-based reservoir computing system.[30]

2. NUMERICAL IMPLEMENTATION OF RESERVOIR COMPUTING

2.1 Delay-based reservoir computing

Semiconductor lasers with delayed feedback rely on a time-multiplexing approach to implement reservoir computing.[19] This delay-based technique has been implemented in several types of electronic or photonic reservoirs.[19,21–23] Fig. 1 shows the topology of a photonic delay-based RC using a single mode semiconductor laser as non-linear node, which will be studied in this paper, and consists of an input layer, reservoir and output layer. In the input layer, we optically inject the discrete input data u_k, with k the index of the data sample, via an input configuration which we will vary in this work. Due to the time-multiplexing, we need to make use of a preprocessing mask $m(t)$ before injecting the input data into the reservoir. In this paper, this mask is created by randomly choosing N values, from following 5 sublevels: $\left[0, \frac{1}{4}, \frac{1}{2}, \frac{3}{4}, 1\right]$. The mask is kept piecewise constant over the randomly selected sublevels, with each interval having a duration θ, the node separation. This piecewise constant segment is then repeated such that the mask is periodic with period $N\theta$, with N the number of virtual nodes in the system. The injection of the input samples u_k is handled numerically in the following procedure. Every data sample is first stretched to a time interval equal to $N\theta$ resulting in a piecewise constant continuous signal $u(t)$. Subsequently, we multiply this signal $u(t)$ with the mask $m(t)$ resulting in a masked data signal $S(t)$. After multiplying this masked data signal with an amplitude (and possibly a bias), it is sent to the reservoir.

The reservoir itself consists of a semiconductor laser (SL) with optical feedback with a delay τ. Note that in this paper, we assume τ and the period of the mask matched, i.e. $\tau = N\theta$. A mismatch between these two can be introduced, as in e.g. Ref.,[5,31–33] which can improve the performance of RCs. However, in this work, we do not consider such a mismatch here for simplicity. The reason for this is that the value of such a mismatch would need to be scanned to further optimize performance. This improvement in performance is expected to be equally applicable to any of the systems which we consider here and would not change the relative differences between them. After the signal passes through the reservoir, the output state, $\mathbf{A}$, is sent to the output layer. The RC's output is then calculated as a linear combination of the node states using (trained) output weights $\mathbf{w}$.[9,18]

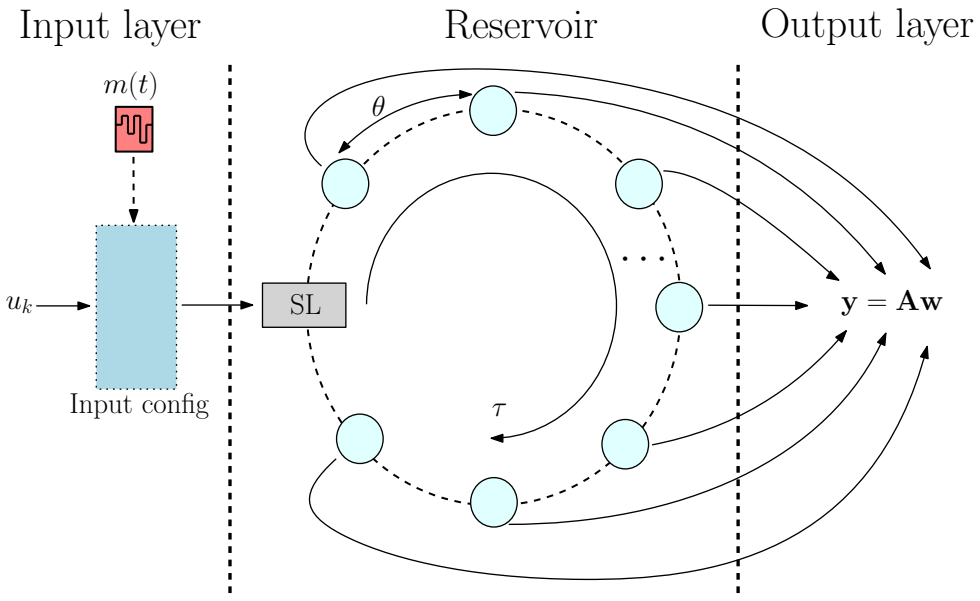

Figure 1: Illustration of a delay-based RC system using a semiconductor laser (SL), with input data u_k, mask $m(t)$, nodal separation θ and delay time τ. The light blue circles represent the virtual nodes and the output layer is defined by the reservoir output $\mathbf{A}$ and output weights $\mathbf{w}$.

We use the intensity of the nodes as output of the reservoir. We can find the output weights $\mathbf{w}$ corresponding to the N nodes of the reservoir in the training phase. In order to achieve this, we use the output of the RC

system $\mathbf{A}$, which represents the node responses to the training input data, and the expected target data $\mathbf{y}^{train}$. In practice, the weights $\mathbf{w}$ can be retrieved by minimizing the squared error $E_{sq}(\mathbf{w})$ between the predicted value for the target data $\hat{\mathbf{y}}^{train}$ and the expected target data points $\mathbf{y}^{train}$.

We have used the real Moore–Penrose pseudoinverse (denoted by the symbol †)

$$\mathbf{w} = \mathbf{A}^{\dagger}\mathbf{y}^{train}. \tag{1}$$

Because of the presence of internal noise in the reservoir, we do not use any regularization methods. Once the weights have been found in the training phase, we test how the RC performs on unseen data, which is referred to as the testing phase. In order to quantify this performance, we use the normalized mean squared error (NMSE) between the expected output $\mathbf{y}^{test}$ and predicted output $\hat{\mathbf{y}}^{test}$, unless indicated differently.

2.2 Numerical implementation of our RC system and the input configurations

The delay-based RC system with a single-mode semiconductor laser as non-linear node, can be accurately modeled using rate-equations[34]

$$\frac{dE(t)}{dt} = \frac{1}{2}(1+i\alpha)\xi n(t)\,E(t) + \eta E(t-\tau)e^{-i\Omega_0\,\tau} + \tilde{F}_\beta + \mu E_{inj}(t) \tag{2}$$

$$\frac{dn(t)}{dt} = \Delta J - \frac{n(t)}{\tau_c} - \left[g + \xi n(t)\right]\left|E(t)\right|^2, \tag{3}$$

where $E(t)$ and $n(t)$ are the complex valued electric field of the laser and the excess amount of available carriers (both dimensionless). α represents the linewidth enhancement factor, and ξ and g the differential gain and threshold gain. Parameters η and μ are the feedback rate and the injection rate. ΔJ represents the excess pump current rate, and is defined as $\Delta J = I_{thr}\Delta I/e$, where I_{thr} is the threshold pump current, e the elementary charge and ΔI the dimensionless pump current excess, $\Delta I = (I - I_{thr})/I_{thr}$. We use a single feedback phase, which is not varied in our work, $\Omega_0\,\tau = 0$. $\tilde{F}_\beta$ represents complex Gaussian white noise to simulate the spontaneous emission noise strength. $\tilde{F}_\beta$ has a zero mean and autocorrelation equal to $< \tilde{F}(t)\tilde{F}(t')^* >= \beta/\tau_c\,\delta(t-t')$, where β controls the spontaneous emission noise and where τ_c is the carrier lifetime. Furthermore, the input data is injected through an optical input signal $E_{inj}(t)$ with the same wavelength as the free running laser, i.e. the injection frequency detuning is therefore equal to zero and not varied in this work. Following previous work in Ref.,[35] we have chosen a value of 20 ps as the standard value for the node separation.[26] Table 1 contains a summary of the parameters of above equations, with their respective standard values. Unless stated otherwise, we keep these parameters fixed to their standard value.

In Fig. 2, we show the different input configurations which we have considered and which were numerically implemented in the input layer of Fig. 1. The first configuration is shown in Fig. 2(a) and consists of a Mach-Zehnder modulator (MZM), which is used to modulate the output beam of a semiconductor laser using the masked data. The second configuration uses only a phase modulator to inject the data, as shown in Fig. 2(b). The optical input signal $E_{inj}(t)$ generated by each of the input configurations shown in Fig. 2 is subsequently sent to the reservoir.

In order to simulate the injection of data in Eq. (2), we specify the term $E_{inj}(t)$:

$$E_{inj}(t) = \begin{cases} \epsilon\left(e^{\frac{i}{2}B_{MZM}(t)} + e^{-\frac{i}{2}B_{MZM}(t)}\right) & \text{for balanced MZM} \quad (4) \\ \tilde{\epsilon}\,e^{iB_{PM}(t)} & \text{for PM} \quad (5) \end{cases}$$

The terms $B_j(t)$ ($j \in \{MZM, PM\}$) represent the masked time-dependent modulator signal which is used as input for the different input configurations of the RC system. These terms are directly related to the voltages $V_j(t)$ in Fig. 2 through $B_j(t) = \pi V_j(t)/(2V_\pi)$, where V_π is the voltage that results in a π phase-shift in the arms of the modulators. Note that the injected intensity $|E_{inj}(t)|^2$ in Eq. (4) is time-dependent, while this is not the case for Eq. (5). Therefore, we have replaced ϵ by $\tilde{\epsilon}$ in Eq. (5), such that we can set the time-averaged

Table 1: Parameters, and their respective values, which are used in the simulations, unless stated otherwise.

Parameter	Symbol	Standard value
Amount of virtual nodes (i.e. neurons)	N	200
Node separation	θ	20 ps
Linewidth enhancement factor	α	3
Threshold gain	g	$1\,\mathrm{ps}^{-1}$
Differential gain	ξ	$5 \times 10^{-9}\ \mathrm{ps}^{-1}$
Spontaneous emission noise factor	β	≈ 100
Carrier lifetime	τ_c	1 ns
Threshold pump current	I_{thr}	16 mA
Excess pump current rate	ΔJ	$1.02 \times 10^5\ \mathrm{ps}^{-1}$
Feedback rate	η	$7.8\,\mathrm{ns}^{-1}$
Injection rate	μ	$98.1\,\mathrm{ns}^{-1}$
Amplitude of injected field	ϵ	100
Feedback phase mismatch	$\Omega_0\,\tau$	0
Modulation amplitude of MZM	A_{MZM}	$\frac{\pi}{2}$
Bias voltage of MZM	Φ_{MZM}	$\frac{\pi}{4}$
Modulation amplitude of PM	A_{PM}	Variable
Bias voltage of PM	Φ_{PM}	0

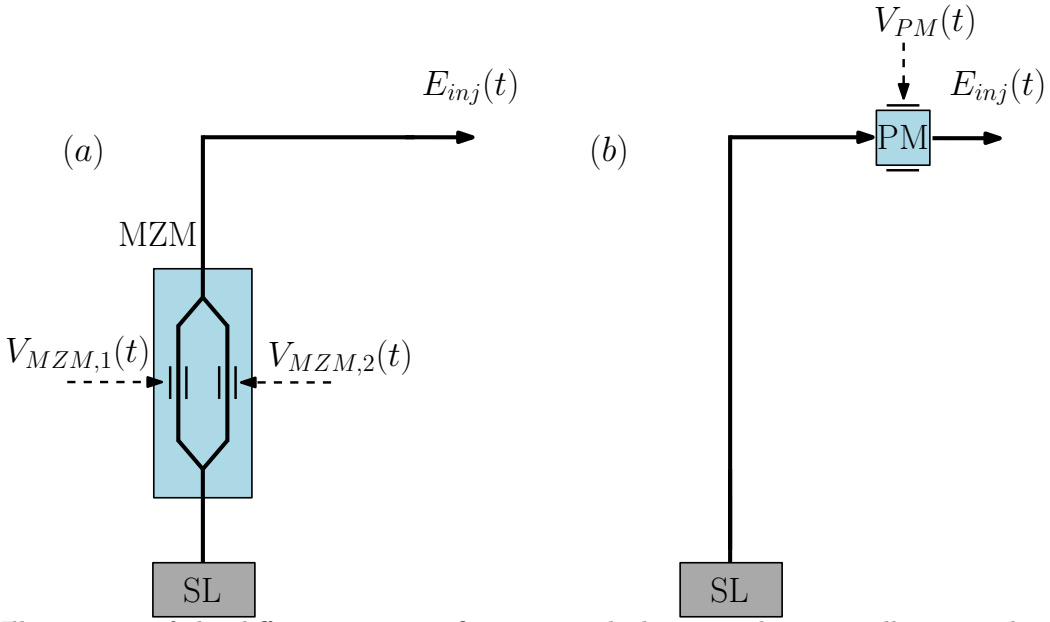

Figure 2: Illustrations of the different input configurations which are used to optically inject the input data u_k, starting from the beam emitted by a semiconductor laser (SL): the balanced MZM only (a) and the phase modulator (b), with their corresponding voltages $V_j(t)$.

energy in $E_{inj}(t)$ equal for all configurations. This $\tilde{\epsilon}$ factor is calculated as the product of ϵ and the time average of the modulus of $E_{inj}(t)$, as present in Eq. (4) and allows for a fair comparison between the different input configurations.

We define the modulator signal $B_j(t)$, corresponding to input configuration j, from the masked data signal $S_j(t)$ using an amplitude A_j and bias Φ_j,

$$B_j(t) = A_j\, S_j(t) + \Phi_j. \tag{6}$$

In order to compare our results for tasks which have different ranges for their input data, we will introduce in our discussions the range of B_j, marked by ΔB_j.

For the simulations of our delay-based RC system we numerically integrate the rate-equations (2)-(3), with the input configurations defined in Eqs. (4)-(5).[30]

3. NUMERICAL RESULTS

3.1 RC performance on Santa Fe task for different input configurations

In order to compare the performance of the different input configurations, we use a one-step ahead time-series prediction task. The input dataset used for this task is the Santa Fe dataset, which consists of just over 9000 data points sampled from a far-IR laser in a chaotic regime.[36] The goal is to find the input configuration which results in the lowest error, and thus the best performance for this particular task with the given reservoir parameters. Typical values for the NMSE for the Santa Fe one-step ahead predictions via simulations of RC systems are around 0.01.[26,37]

We have taken the first 3000 data samples from the discrete Santa Fe dataset, u_k^{train}, where $k \in \{1, \ldots, 3000\}$, as the training set in the RC system. As test set u_k^{test}, we have taken the next 1000 data samples, as done in Ref.[38] Before injecting the signals, all of the Santa Fe data was normalized over the whole dataset, so that for both training and testing, $u_k \in [0,1]$. We have repeated each numerical experiment 10 times, each with different mask realizations, from which we calculate the average NMSE and its standard deviation. We use the standard deviation as the error bars in subsequent figures.

If we consider a balanced MZM as input configuration, we find an NMSE $= 0.134 \pm 0.044$. This result is in agreement with typical NMSE values found in literature.[26,37] This is shown in Fig. 3, where we show the NMSE versus the total range of the phase modulator signal ΔB_{PM} for different input configurations. In this figure, we have indicated the performance of the balanced MZM as a horizontal line.

We observe that for the input configuration consisting of a PM that the NMSE initially decreases when increasing ΔB_{PM}, then reaches an optimal point (lowest) and again increases for larger ΔB_{PM}.

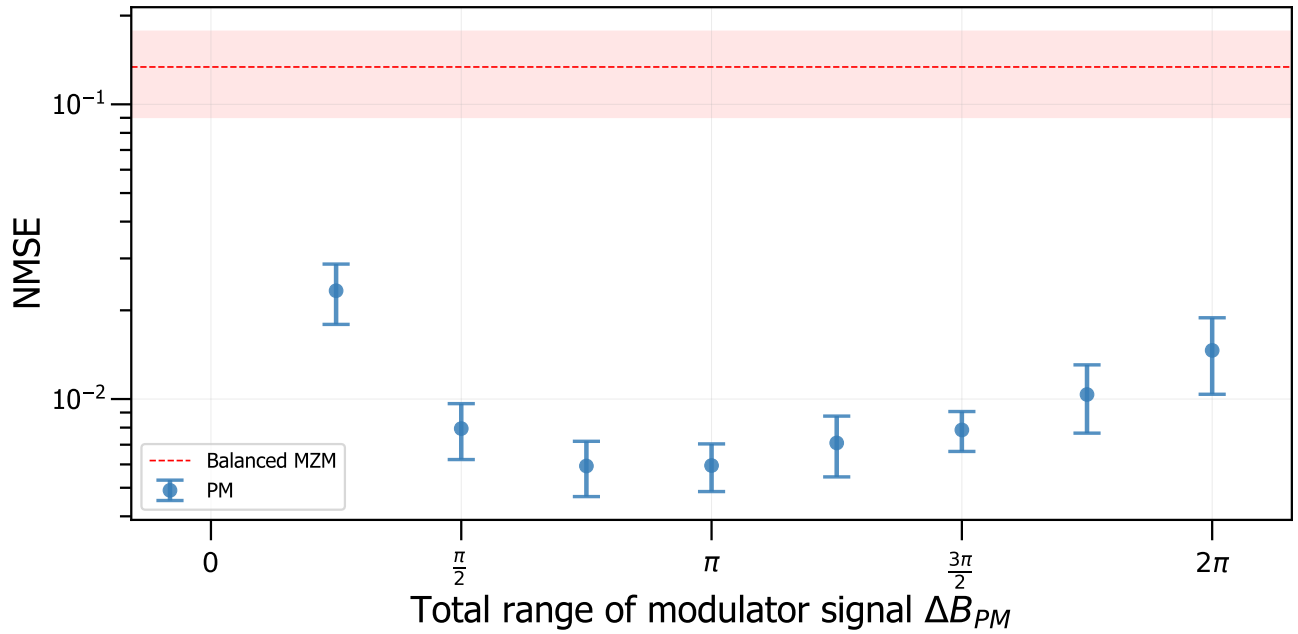

Figure 3: NMSE in function of the total range ΔB_{PM} of the phase modulator signal for one-step ahead prediction of Santa Fe data.

As we achieve a large improvement by adding a phase modulator, the question can be raised whether an MZM is required at all to obtain good RC performance. Ultimately, this allows for a simpler input configuration that

only uses a phase modulator. We observe in Fig. 3 that the input configuration where only a PM is used results in the best mean NMSE for the given reservoir. This shows that by replacing the MZM with a PM for the input configuration, and thus reducing the complexity of the input system, an improved performance can be achieved.

In Fig. 3, we observe that the lowest NMSE values occur for input configurations with PMs around the broad range of $\Delta B_{PM} = \frac{\pi}{2}$ to $\Delta B_{PM} = \pi$. Therefore, we achieve an improvement in the performance within this large ΔB_{PM} range. This optimal NMSE can be explained by two factors. For small ΔB_{PM} (around $\frac{\pi}{4}$), the system is limited by noise that obstructs the masked data, so that it becomes difficult for the system to distinguish noise from different sublevel mask values. For large ΔB_{PM}, the phase modulated signal will stand to wrap on itself. Both of these phenomena will have a negative effect on the achieved performance and explain the existence of the optimal range in the modulator signal range ΔB_{PM}.[30]

4. CONCLUSION

We have numerically investigated the effect of modulating the phase when optically injecting data, with the goal of improving delay-based reservoir computing with semiconductor lasers. Using a phase modulator to inject the signal into the reservoir, with a well-chosen modulation amplitude, resulted in an improved performance compared to literature. We therefore conclude that modulating the phase of the injected signal strongly increases the performance of optical reservoir computing for the one-step ahead prediction Santa Fe task, both performance-wise as well as in simplicity for implementation.

ACKNOWLEDGMENTS

We acknowledge financial support of the FWO (Fonds Wetenschappelijk Onderzoek - Vlaanderen) under grants G006020N, G028618N and G029519N. Additionally, we would like to thank Bryan Kelleher for the inspiring discussions.

REFERENCES

[1] Alsheikh, M. A., Niyato, D., Lin, S., Tan, H.-P., and Han, Z., "Mobile big data analytics using deep learning and apache spark," *IEEE network* **30**(3), 22–29 (2016).
[2] Verstraeten, D., Schrauwen, B., Stroobandt, D., and Van Campenhout, J., "Isolated word recognition with the liquid state machine: a case study," *Information Processing Letters* **95**(6), 521–528 (2005).
[3] Salehi, M. R., Abiri, E., and Dehyadegari, L., "An analytical approach to photonic reservoir computing–a network of SOA's–for noisy speech recognition," *Optics Communications* **306**, 135–139 (2013).
[4] Verstraeten, D., Schrauwen, B., and Stroobandt, D., "Reservoir-based techniques for speech recognition," in [*The 2006 IEEE International Joint Conference on Neural Network Proceedings*], 1050–1053, IEEE (2006).
[5] Paquot, Y., Duport, F., Smerieri, A., Dambre, J., Schrauwen, B., Haelterman, M., and Massar, S., "Optoelectronic reservoir computing," *Scientific reports* **2**(1), 1–6 (2012).
[6] Jaeger, H. and Haas, H., "Harnessing nonlinearity: Predicting chaotic systems and saving energy in wireless communication," *Science* **304**(5667), 78–80 (2004).
[7] Skibinsky-Gitlin, E. S., Alomar, M. L., Isern, E., Roca, M., Canals, V., and Rossello, J. L., "Reservoir computing hardware for time series forecasting," in [*2018 28th International Symposium on Power and Timing Modeling, Optimization and Simulation (PATMOS)*], 133–139, IEEE (2018).
[8] Canaday, D., Griffith, A., and Gauthier, D. J., "Rapid time series prediction with a hardware-based reservoir computer," *Chaos: An Interdisciplinary Journal of Nonlinear Science* **28**(12), 123119 (2018).
[9] Van der Sande, G., Brunner, D., and Soriano, M. C., "Advances in photonic reservoir computing," *Nanophotonics* **6**(3), 561–576 (2017).
[10] De Lima, T. F., Shastri, B. J., Tait, A. N., Nahmias, M. A., and Prucnal, P. R., "Progress in neuromorphic photonics," *Nanophotonics* **6**(3), 577–599 (2017).
[11] Sackesyn, S., Ma, C., Dambre, J., and Bienstman, P., "Experimental realization of integrated photonic reservoir computing for nonlinear fiber distortion compensation," *Optics Express* **29**(20), 30991–30997 (2021).
[12] Vandoorne, K., Dambre, J., Verstraeten, D., Schrauwen, B., and Bienstman, P., "Parallel reservoir computing using optical amplifiers," *IEEE transactions on neural networks* **22**(9), 1469–1481 (2011).
[13] Vandoorne, K., Dierckx, W., Schrauwen, B., Verstraeten, D., Baets, R., Bienstman, P., and Van Campenhout, J., "Toward optical signal processing using photonic reservoir computing," *Optics express* **16**(15), 11182–11192 (2008).
[14] Takano, K., Sugano, C., Inubushi, M., Yoshimura, K., Sunada, S., Kanno, K., and Uchida, A., "Compact reservoir computing with a photonic integrated circuit," *Optics express* **26**(22), 29424–29439 (2018).

[15] Brunner, D. and Fischer, I., "Reconfigurable semiconductor laser networks based on diffractive coupling," *Optics letters* **40**(16), 3854–3857 (2015).
[16] Robertson, J., Hejda, M., Bueno, J., and Hurtado, A., "Ultrafast optical integration and pattern classification for neuromorphic photonics based on spiking VCSEL neurons," *Scientific reports* **10**(1), 1–8 (2020).
[17] Tait, A. N., Nahmias, M. A., Shastri, B. J., and Prucnal, P. R., "Broadcast and weight: an integrated network for scalable photonic spike processing," *Journal of Lightwave Technology* **32**(21), 4029–4041 (2014).
[18] Appeltant, L., Soriano, M. C., Van der Sande, G., Danckaert, J., Massar, S., Dambre, J., Schrauwen, B., Mirasso, C. R., and Fischer, I., "Information processing using a single dynamical node as complex system," *Nature communications* **2**(1), 1–6 (2011).
[19] Harkhoe, K., Verschaffelt, G., Katumba, A., Bienstman, P., and Van der Sande, G., "Demonstrating delay-based reservoir computing using a compact photonic integrated chip," *Optics express* **28**(3), 3086–3096 (2020).
[20] Van der Sande, G., Harkhoe, K., Katumba, A., Bienstman, P., and Verschaffelt, G., "Integrated photonic delay-lasers for reservoir computing," in [*Physics and Simulation of Optoelectronic Devices XXVIII*], **11274**, 112740D, International Society for Optics and Photonics (2020).
[21] Soriano, M. C., Ortín, S., Keuninckx, L., Appeltant, L., Danckaert, J., Pesquera, L., and Van der Sande, G., "Delay-based reservoir computing: noise effects in a combined analog and digital implementation," *IEEE transactions on neural networks and learning systems* **26**(2), 388–393 (2014).
[22] Toutounji, H., Schumacher, J., and Pipa, G., "Optimized temporal multiplexing for reservoir computing with a single delay-coupled node," in [*The 2012 International Symposium on Nonlinear Theory and its Applications (NOLTA 2012)*], (2012).
[23] Larger, L., Baylón-Fuentes, A., Martinenghi, R., Udaltsov, V. S., Chembo, Y. K., and Jacquot, M., "High-speed photonic reservoir computing using a time-delay-based architecture: Million words per second classification," *Physical Review X* **7**(1), 011015 (2017).
[24] Zeng, Q., Wu, Z., Yue, D., Tan, X., Tao, J., and Xia, G., "Performance optimization of a reservoir computing system based on a solitary semiconductor laser under electrical-message injection," *Applied Optics* **59**(23), 6932–6938 (2020).
[25] Brunner, D., Soriano, M. C., Mirasso, C. R., and Fischer, I., "Parallel photonic information processing at gigabyte per second data rates using transient states," *Nature communications* **4**(1), 1–7 (2013).
[26] Nguimdo, R. M., Verschaffelt, G., Danckaert, J., and Van der Sande, G., "Fast photonic information processing using semiconductor lasers with delayed optical feedback: Role of phase dynamics," *Optics express* **22**(7), 8672–8686 (2014).
[27] Sozos, K., Mesaritakis, C., and Bogris, A., "Reservoir computing based on mutually injected phase modulated lasers: A monolithic integration approach suitable for short-reach communication systems," in [*Optical Fiber Communication Conference*], W6A–4, Optical Society of America (2021).
[28] Nakayama, J., Kanno, K., and Uchida, A., "Laser dynamical reservoir computing with consistency: an approach of a chaos mask signal," *Optics express* **24**(8), 8679–8692 (2016).
[29] Cai, Q., Guo, Y., Li, P., Bogris, A., Shore, K. A., Zhang, Y., and Wang, Y., "Modulation format identification in fiber communications using single dynamical node-based photonic reservoir computing," *Photonics Research* **9**(1), B1–B8 (2021).
[30] Bauwens, I., Harkhoe, K., Bienstman, P., Verschaffelt, G., and Van der Sande, G., "Influence of the input signal's phase modulation on the performance of optical delay-based reservoir computing using semiconductor lasers," *Optics Express* **30**(8), 13434–13446 (2022).
[31] Duport, F., Schneider, B., Smerieri, A., Haelterman, M., and Massar, S., "All-optical reservoir computing," *Optics express* **20**(20), 22783–22795 (2012).
[32] Duport, F., Smerieri, A., Akrout, A., Haelterman, M., and Massar, S., "Fully analogue photonic reservoir computer," *Scientific reports* **6**(1), 1–12 (2016).
[33] Stelzer, F., Röhm, A., Lüdge, K., and Yanchuk, S., "Performance boost of time-delay reservoir computing by non-resonant clock cycle," *Neural Networks* **124**, 158–169 (2020).
[34] Lenstra, D. and Yousefi, M., "Rate-equation model for multi-mode semiconductor lasers with spatial hole burning," *Optics express* **22**(7), 8143–8149 (2014).
[35] Harkhoe, K. and Van der Sande, G., "Delay-based reservoir computing using multimode semiconductor lasers: Exploiting the rich carrier dynamics," *IEEE Journal of Selected Topics in Quantum Electronics* **25**(6), 1–9 (2019).
[36] Weigend, A. S. and Gershenfeld, N. A., "The Santa Fe time series competition data," (1991).
[37] Soriano, M. C., Ortín, S., Brunner, D., Larger, L., Mirasso, C. R., Fischer, I., and Pesquera, L., "Optoelectronic reservoir computing: tackling noise-induced performance degradation," *Optics express* **21**(1), 12–20 (2013).

[38] Harkhoe, K. and Van der Sande, G., "Task-independent computational abilities of semiconductor lasers with delayed optical feedback for reservoir computing," in [*Photonics*], **6**(4), 124, Multidisciplinary Digital Publishing Institute (2019).